Analytical and Experimental Investigation of overall Heat Loss Coefficient for Single Non-Evacuated Tube Solar Thermal Receiver

Saroj Kumar Singh[1], Kishan Konannarvar[1], S. B. Kedare[1], and S.V. Prabhu[2*]
[1]Department of Energy Science and Engineering
[2]Department of Mechanical Engineering,
Indian Institute of Technology Bombay, Mumbai, Maharashtra, India, 400076

Abstract

Concentrating Solar Power (CSP) using Linear Fresnel Reflectors (LFR) is a promising technology for harnessing power from the sun. The tubular receiver in LFR has a significant impact on its efficient performance. In the present work, thermal characteristics of four different configurations and dimensions of absorber and surrounded by the concentric glass tube are studied. The experimental investigations are employed to characterise the non-evacuated LFR receivers using the overall heat loss coefficient (HLC). The absorber tube wall temperatures are achieved between 50°C and 215°C which is typically achieved in LFR. Influence of the angular gap ratio (0.26, 0.625, 0.8 and 1.4) on the overall HLC is investigated (Annular gap ratio is the ratio of annular gap between absorber and glass tube and the outer diameter of the absorber tube). The overall HLC increases with increase in the absorber wall temperature. For a given absorber wall temperature, the overall HLC increases with the increase in the annular gap ratio. The overall HLC obtained from an analytical model is reasonably agree with the experimental results. An empirical correlation for overall HLC as a function of annular gap ratio and difference of absorber temperature and ambient temperature is proposed.

Keywords: Overall heat loss coefficient, Single tube non-evacuated receiver, Linear Fresnel Reflector, Concentrating Solar Power (CSP), Annular gap ratio

1. Introduction

Solar thermal energy is an attractive option as a renewable energy source for power generation. Solar energy, present on the Earth's surface, exists predominantly in a diffused form. Concentrating Solar Power (CSP) technologies focus incident solar radiation onto a receiver surface which is cooled by an HTF. The fluid heated to high temperature can be used to run a turbine to generate power or provide heat or steam for industrial processes for decarbonization. In an LFR solar collector system, the solar radiation is focussed by the reflectors on the ground onto a line which is the common focal line of the reflectors. It uses an array of flat or slightly curved mirrors to concentrate the incoming solar radiation onto a line focus. The LFR technology has a few advantages over PTC [1 – 4]. The LFRs may differ in the design of receivers [3]. The receiver may consist of multiple absorber tubes or a single absorber tube. A significant proportion of the solar incident radiation is concentrated on the absorber tube and subsequently transferred to the working fluid flowing through it. The remaining part of the energy is lost to the environments. The absorber can lose heat to the ambient through all the modes of heat transfer: conduction, natural convection and radiation. The overall HLC, calculated on the basis of absorber tube temperature and absorber tube surface area, is used to characterise the heat loss from the receiver. Factors like the size of the receiver design, surface coating, absorber temperature and presence of gas in the annulus affects the overall HLC. Due to the significant role of the heat loss in the thermal performance of the solar plant, a huge emphasis is laid on the study of the same in linear solar receivers.

Singh *et al*. [5] conducted experimental research to investigate how the overall HLC changes with absorber temperature in a trapezoidal cavity. Their study was conducted under laboratory conditions, exploring various absorber shapes, surface coatings, and the number of glass tubes. Larsen *et al.* [6] reported experimental studies on the steady-state heat loss from a linear trapezoidal cavity receiver with five absorber tubes. The heat loss calculations indicated that about 91% of the heat loss occurred from the surface of the glass window at the aperture covering at the bottom of the cavity receiver and rest 9% was loss through the secondary reflector by conduction which is at 200℃. Out of the total heat lost at the aperture surface, 88% was determined to have been lost by radiation and the rest 12% being the convective loss from the aperture cover. Numerical studies on optical performance and overall HLC of a trapezoidal cavity receiver for a fixed collector geometry were carried out by Facão and Oliveira [7]. Sahoo *et al*. [8] numerically studied heat loss in a trapezoidal cavity with eight tubes.

10.18086/swc.2025.01.02 Available at http://proceedings.ises.org

A theoretical analysis of Solar-Mundo Fresnel collector [1] showed that thermal performance of Fresnel collector with single tube receiver and secondary reflector is 70% of Parabolic Trough Collector based on aperture area. However, the cost of production of electricity using the Fresnel collector was found to be 10% lower than that of PTC. Balaji *et al*. [9] and Reddy *et al.* [10] investigated numerically the thermal loss for a single tube receiver with secondary parabolic reflector of an LFR absorber tube enclosed in a concentric glass cover. In comparison to non – evacuated absorber tube, about $65\% - 70\%$ reduction in overall heat loss (radiation and convection) for (absorber surface emissivity of 0.075) was obtained when the absorber tube was placed in an evacuated glass tube. The radiation mode of heat transfer was found to dominate convection heat transfer by $60\% - 92\%$ in the evacuated receiver case. Ratzel *et al*. [11] explored techniques for reducing thermal losses in a tubular receiver. The losses were modelled analytically. Gee *et al*. [12] evaluated the annual energy delivery of parabolic trough using models for thermal and optical characteristics. Montes *et al.* observed that the evacuated tube receivers have 65% to 70% low thermal losses, but are comparatively $10\% - 12\%$ more costly and are susceptible to loss of vacuum resulting in significant reduction in performance. The loss of vacuum may occur either due to damage of glass to metal seal and breakage of enveloping glass tube in the evacuated annular space [13].

In the present work, overall HLC based on annular gap ratio (δ^*) for different configurations of test section are studied experimentally which is not done earlier. Heat loss measurements in a non-evacuated tube receiver are carried out. In this study, the overall HLC of experimental results are compared with analytical results. Influence of annular gap ratio on the overall HLC is presented. The objectives of the present work are as follows

1) Develop an analytical model for the non-evacuated single-tube receiver under constant heat flux to estimate overall heat loss coefficient (HLC) by considering convective, radiative, and conductive heat losses
2) Validate the analytical model using experimental HLC data at different temperatures and use it to determine the individual contributions of convection, radiation, and conduction to total heat loss.

2. Experimental Setup and Procedure

An experimental setup is fabricated to study the effect of the absorber and glass tube diameters on the overall heat loss coefficient representing a single non-evacuated tube solar thermal receiver. The layout of the experimental configuration is shown in Fig.1.

The enlarged view of the given configuration is represented in Fig. 2. The experimental setup consists of a SS tube enclosed concentrically in a borosilicate glass tube. The glass tube is sandwiched between copper flanges on either end. The stainless-steel tube is then brazed to circular copper flanges at either end. Silicone gaskets are used in between glass tube and the copper flanges. Brazing and silicone gaskets are employed to ensure that there is no leakage of the air trapped in the circular space created between the glass tube and the SS tube. Joule heating is used to supply the heat to the receiver test section. AC power is supplied to the stainless-steel tube through a step-down transformer (2 kW). K-type thermocouples are employed for temperature measurement on both the SS tube and the glass tube. Six thermocouples are used for stainless steel tube for temperature measurements which were located equidistant from each other. Thermocouples are attached to the SS tube at the uppermost point and the lowermost point at each of three axial locations. The points T_7 through T_{12} in Fig. 2 are the positions where thermocouples are placed to measure the temperature of the absorber tube wall. Similarly, these thermocouples are placed at two diametrically opposite points at identical axial positions along the outer surface of the glass tube. These are shown as points T_1 through T_6 in Fig. 2. The voltages (in mV) from the thermocouples are received by a DAS (Agilent Keysight 34972a).

The use of multiple thermocouples on the SS tube provides the extent of uniform distribution of temperature over the tube. The current and voltage across the test section is measured with the help of clamp meter and multi-meter respectively. The copper flanges on both ends are thermally insulated by wrapping glass wool over them. Once the stainless−steel tube is begun to be heated by supplying current through it, the temperatures are recorded at every 10 seconds. The design parameters, annular gap, range of experimental measured temperature and heat flux for four different configurations are shown in the Table 1.

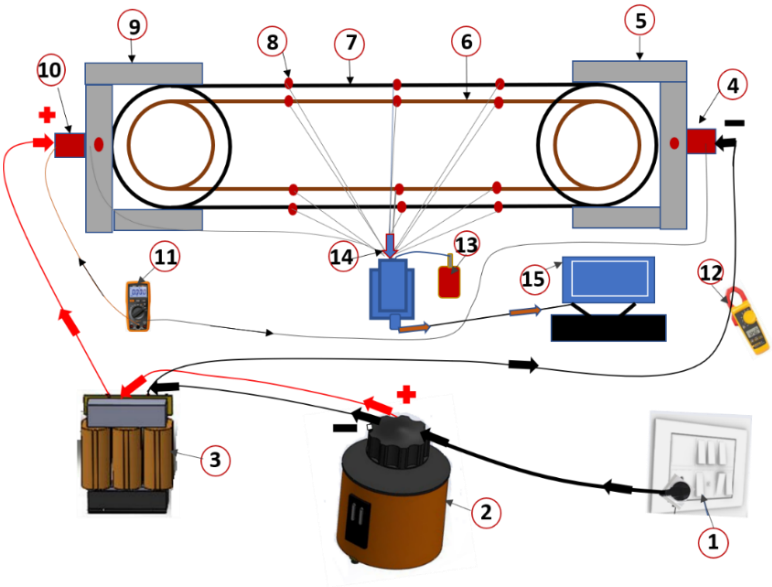

(1) Power supply board (2) Variac (3) Transformer (2 kW) (4) Negative terminal (5) Copper flange (6) Absorber tube (7) Concentric glass tube (8) Thermo-couple (9) Copper flange (10) Positive terminal (11) Clampmeter (12) Multimeter (13) Data logger (14) Red dot shows all thermo-couple connection in data logger (15) Laptop

Fig.1 Schematic of experimental set-up of absorber and concentric glass tube for non-evacuated tube receiver

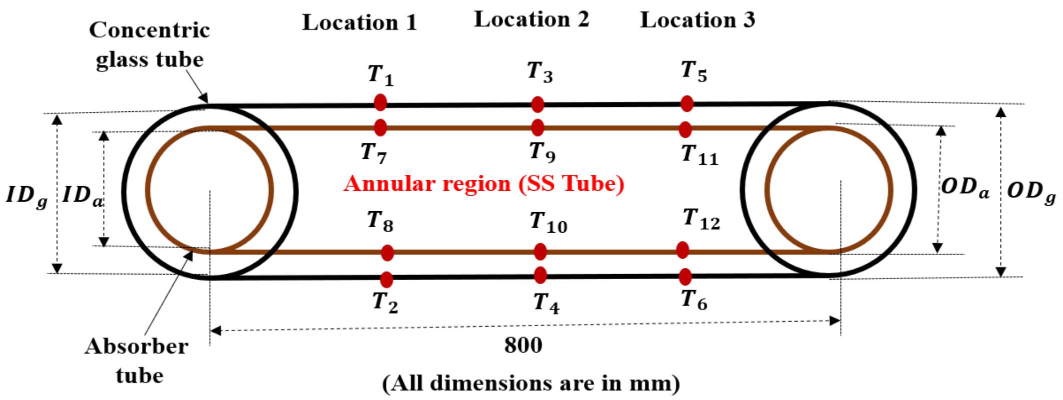

Fig. 2 Schematic of absorber and concentric glass tube with thermocouple locations

Table 1. Design parameters, annular gap, range of experimental measured temperature and heat flux

No. of test section	OD_a (mm)	ID_a (mm)	OD_g (mm)	ID_g (mm)	δ (mm) $\left(\frac{ID_g - OD_a}{2}\right)$	(T_a) (°C)	q'' (W/m^2)
1	25	22.5	46	38	6.5	63 − 193	221 − 2013
2	10	6	32	26	8	96 − 212	687 − 3123
3	10	7.5	46	38	14	96 − 202	816 − 3000
4	10	7.5	28.5	22.5	6.25	54 − 192	202 − 2515

3. Data Reduction

3.1. Experimentally determining the overall heat loss coefficient

In the present study, the heat is supplied to the inner tube in the form of resistance heating of the stainless−steel (SS) tube. At steady state condition, the heat supplied to the inner SS tube is equal to the heat lost to the ambient from absorber tube. The heat supplied ($\dot{Q}_{supply} = V \times I = \dot{Q}_{ao}$) to the absorber tube is calculated by Eq. (1).

$$\dot{Q}_{ao} = V \times I \qquad (1)$$

where, $\dot{Q}_{ao}$ is total heat transfer from inner tube to ambient. The overall HLC (U_L) is determined using Eq. (2).

$$U_L = \frac{\dot{Q}_{ao}}{A_a(T_a - T_{amb})} \tag{2}$$

where, A_a, T_a, and T_{amb} are the outer surface area of absorber tube, average temperature of absorber tube and ambient temperature, respectively. The average temperature of absorber tube is obtained by measuring the inner tube wall temperature of absorber at six points occupying three axial locations and taking their average value. It is calculated by the Eq. (3)

$$T_a = \left(\frac{\sum_{i=7}^{i=12} T_i}{6}\right) \tag{3}$$

The uncertainties in both the measured and calculated parameters are assessed using the Moffat method [14]. Table 2 presents the uncertainties in experimental parameters. The uncertainty in the diameter

Table 2. uncertainties in different experimental parameters

Parameters	Uncertainty
Outer and inner diameter of absorber tube, OD and ID $(6 - 46\ mm)$	$0.5\ mm$
Length of the test section, L $(800\ mm)$	$1\ mm$
Supply voltages, V (0.40 volts to 2 volts)	0.0118 to 7.3
Supply current, I (40 A to 150 A)	1.0 to 9.6
Reading in thermocouples temperature	0.5 ℃
Overall heat loss coefficient (U_L)	2.5−12.73 %
Heat Flux (q'')	2.5−11.4 %

3.2 Analytical approach for estimating the overall heat loss coefficient (HLC)

The experimental results serve to validate the derived analytical model for estimating the overall HLC of the absorber tubes. The HLC are estimated analytically by considering the heat loss from absorber tube to the ambient surrounded by glass tube. The experimental overall HLC (U_L) is evaluated by using the Eq. (2). The different heat transfer modes through which the heat is lost to the ambient are shown in Fig. 3.

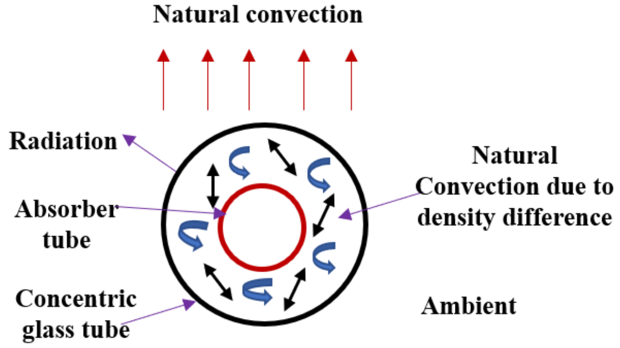

Fig. 3 Modes of transfer of heat in the tubular receiver

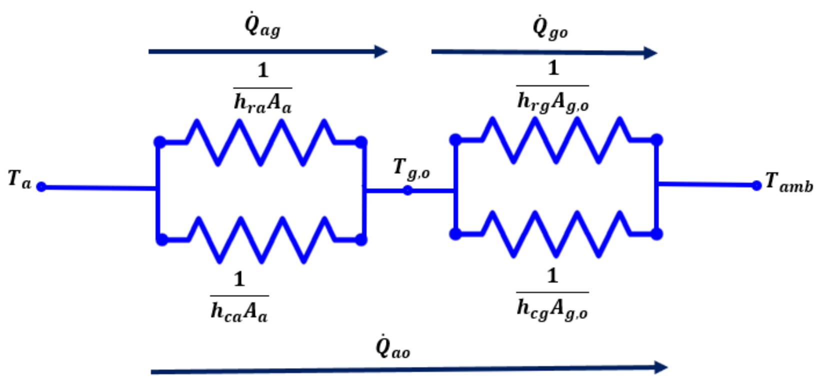

Fig. 4 Electrical network diagram for the transfer of heat rate from absorber tube to the ambient through the glass tube

The analytical prediction of overall HLC is obtained by considering the heat loss from the inner absorber tube to the environment. The first part is the heat loss from the absorber tube to the concentric glass tube. These losses are from the absorber tube to the glass occurs through free convection (natural convection) by the air trapped in the annular space and radiation simultaneously. Similarly, the second part consists of the losses of heat from the glass tube to ambient. The heat initially transferred from the absorber tube to the glass tube is subsequently dissipated to the surrounding environment from the glass tube through free convection and radiation. The losses of heat from the absorber tube to the surrounding environment represents as an equivalent electrical resistance network diagram depicted in Fig. 4. The radiation heat loss between the absorber tube and the glass tube is estimated as radiation heat loss within the space formed by two concentric cylinders whose surfaces are assumed to be grey, diffuse and opaque. The heat transfer through radiation between the absorber and glass inner surface of glass tube is estimated by Eq. (4).

$$\dot{Q}_{rad,ag} = \frac{A_a\,\sigma\,(T_a^4 - T_{g,i}^4)}{\frac{1}{\epsilon_a} + \frac{1-\epsilon_g}{\epsilon_g}\left(\frac{OD_a}{ID_g}\right)} \tag{4}$$

where $\dot{Q}_{rad,ag}$, ϵ_a, ϵ_g, $T_{g,i}$, T_a, OD_a and ID_g are heat transfer rate by radiation from absorber tube to inner surface of glass tube, emissivity of absorber tube, emissivity of concentric glass tube, inner surface of glass tube temperature, average absorber tube temperature, outer diameter of absorber and inner diameter of glass tube, respectively.

Expressing the terms, $(T_a^4 - T_{g,i}^4)\ as\ (T_a^2 + T_{g,i}^2)(T_a + T_{g,i})(T_a - T_{g,i})$

$$\dot{Q}_{rad,ag} = h_{ra}\,A_a(T_a - T_{g,i}) \tag{5}$$

$$h_{ra} = \frac{\sigma\,(T_a^2 + T_{g,i}^2)(T_a + T_{g,i})}{\frac{1}{\varepsilon_a} + \frac{1-\varepsilon_g}{\varepsilon_g}\left(\frac{OD_a}{ID_g}\right)} \tag{6}$$

The heat transfer rate by radiation from absorber tube to inner surface of glass tube and radiation heat transfer coefficient from absorber tube to inner surface of glass tube is calculated by the Eq. (5) and Eq. (6), respectively. The heat loss by the convection from the absorber tube to the inner surface of glass tube (annulus) is calculated by the Eq. (7).

$$\dot{Q}_{conv,ag} = h_{ca}\,A_a(T_a - T_{g,i}) \tag{7}$$

$\dot{Q}_{conv,ag}$ and h_{ca} are the heat transfer rate by convection between the absorber tube and inner surface of glass tube and convective HTC from absorber tube to inner surface of glass tube, respectively. The transfer heat rate from the inner surface of glass tube to the outer surface of glass tube through conduction. The temperature of the outer surface of the glass is measured using thermocouples. The inner glass tube temperature is then estimated by one dimensional heat conduction equation in a cylinder. The temperature gap between the inner and outer surfaces of the concentric glass tube is within a range of 2°C or less. Hence, the conduction heat transfer through the glass tube is neglected and the temperatures of the inner and outer surfaces of the glass tube are considered to be equal ($T_{g,i} \sim T_{g,o}$). The heat loss from the glass tube to ambient also occurs through natural convection and radiation simultaneously. Radiation heat transfer from the glass tube to the ambient is considered as radiation between a small object and a large cavity forming an enclosure. The surfaces are considered as grey, diffuse and opaque. The heat transfer rate by the radiation between the outer glass tube surface and the surrounding environment is estimated by the Eq. (8).

$$\dot{Q}_{rad,go} = A_{g,o}\,\sigma\,\epsilon_g(T_{g,o}^4 - T_{amb}^4) \tag{8}$$

where, $\dot{Q}_{rad,go}$, $A_{g,o}$, $T_{,go}$, σ and ϵ_g are heat transfer by the radiation between the outer glass tube and environment, outer surface area of glass tube, glass tube wall temperature, Boltzmann constant and emissivity of glass tube.

Expressing $(T_{g,o}^4 - T_{amb}^4)\ as\ (T_{g,o}^2 + T_{amb}^2)(T_{g,o} + T_{amb})(T_{g,o} - T_{g,o})$, Eq. 7 can be written as

$$\dot{Q}_{rad,g,o} = h_{rg}\,A_{g,o}(T_{g,o} - T_{amb}) \tag{9}$$

$$h_{rg} = \sigma\,\varepsilon_g(T_{g,o}^2 + T_{amb}^2)(T_{g,o} + T_{amb}) \tag{10}$$

$\dot{Q}_{rad,g,o}$ and h_{rg} are the heat transfer rate by radiation between the glass tube and outer surface of glass tube and radiative HTC from glass tube to ambient is calculated by Eq. (9) and Eq. (10), respectively. The heat transfer rate by the free convection from glass tube to ambient is estimated by Eq. (11).

$$\dot{Q}_{conv,go} = h_{cg}\,A_{g,o}(T_{g,o} - T_{amb}) \tag{11}$$

where, $\dot{Q}_{conv,go}$ and h_{cg} are the heat transfer rate by the free convection from glass tube to ambient and HTC from the glass tube to the ambient, respectively. Based on electrical network circuit diagram as Fig. 4, the transfer of heat rate from absorber tube to the ambient through the glass tube (the cumulative effect of radiation and natural convection contributes to the overall heat loss from the absorber tube to the glass tube) is estimated by Eq. (12).

$$\dot{Q}_{ag} = h_{ra}\, A_a\, (T_a - T_{g,i}) + h_{ca}\, A_a\, (T_a - T_{g,i}) \tag{12}$$

where, $\dot{Q}_{ag}$ is the total heat transfer rate from the absorber tube to glass tube. Similarly, the total heat transfer rate from glass tube to ambient ($\dot{Q}_{g,o}$) is calculated by the Eq. (13).

$$\dot{Q}_{g,o} = h_{rg}\, A_{g,o}(T_{g,o} - T_{amb}) + h_{cg}\, A_{g,o}(T_{g,o} - T_{amb}) \tag{13}$$

$$\dot{Q}_{ao} = \frac{(T_a - T_{amb})}{\dfrac{1}{(h_{ra}\, A_a + h_{ca}\, A_a)} + \dfrac{1}{(h_{rg}\, A_{g,o} + h_{cg}\, A_{g,o})}} \tag{14}$$

From Fig. 4, The net heat transfer rate ($\dot{Q}_{ao}$) from the absorber tube to the surrounding environment is expressed in terms of the overall heat loss coefficient (U_L) in the Eq. (15).

$$\dot{Q}_{ao} = U_L\, A_a(T_a - T_{amb}) \tag{15}$$

Comparing Eq. (14) and Eq. (15),

$$\frac{1}{U_L} = \frac{1}{(h_{ra} + h_{ca})} + \left(\frac{A_a}{A_{g,o}}\right)\left(\frac{1}{h_{rg} + h_{cg}}\right) \tag{16}$$

Eq. (16). gives the overall HLC in terms of convection and radiation HTC. The loss of heat by the convective from the inner tube to the concentric glass tube is estimated by Bejan [15] interpretation of the correlation given by Rathby and Hollands [16]. The total convective heat transfer per unit length between the absorber tube and the glass tube, $q'_{conv,ag}$ is given in Eq. (17). The Rayleigh number (Ra_{ODa}) is calculated based on the outer tube diameter of absorber tube which given by the Eq. (18).

$$q'_{conv,ag} \cong \frac{2.425 k_{air}(T_a - T_{g,i})}{\left[1 + \left(\dfrac{OD_a}{ID_g}\right)^{\frac{3}{5}}\right]^{\frac{5}{4}}} \left(\frac{Pr_{ag} Ra_{ODa}}{0.861 + Pr_{ag}}\right)^{\frac{1}{4}} \tag{17}$$

$$Ra_{Da,o} = \frac{g\beta(T_a - T_{g,i})OD_a^3}{\alpha_{air}\, \gamma_{air}} \tag{18}$$

The thermal properties of air are evaluated as outer temperature of average absorber tube and glass inner tube wall temperature. The correlation given in Eq. (18) can be used for Rayleigh numbers upto 10^7. The lower limit of the Rayleigh number for the applicability of Eq. (18) is reached when the inequality ($ID_g\, Ra_{IDg}^{\frac{-1}{4}}$) $> (ID_g - OD_a)$ is satisfied. The thermal physical properties of the air are evaluated at the average of the absorber tube and the glass tube temperatures. Using Eq. (17), the total heat transfer over the absorber tube length can be determined. The free convection transfer of heat around an iso-thermal horizontal cylinder in a fluid is considered for determining the convection HLC from the glass tube to the ambient. The mean Nusselt number over the surface is expressed by Eq. (19) [17], which is applicable for the whole Prandtl number ranges. The Rayleigh number ($Ra_{ODg,o}$) is calculated based on the outer tube diameter of glass tube which given by the Eq. (20) and their range is shown in the Eq. (21).

$$\overline{Nu}_{conv,ODg} = \left[\frac{0.6 + 0.387 Ra_{ODg}^{\frac{1}{6}}}{\left\{1 + \left(\dfrac{0.559}{Pr_{go}}\right)^{\frac{9}{16}}\right\}^{\frac{8}{27}}}\right]^2 \tag{19}$$

$$Ra_{ODg,o} = \frac{g\beta(T_{g,o} - T_{amb})OD_g^3}{\alpha_{air}\, \gamma_{air}} \tag{20}$$

$$10^{-5} < Ra_{ODg,o} < 10^{12} \tag{21}$$

where, $Pr_{g,o}$ is Prandtl number for heat transfer between the outer glass tube to ambient. The thermal properties of air are evaluated at the mean temperature of concentric glass tube and ambient. The convective heat flux can be determined using Eq. (22).

$$q''_{conv,go} = \frac{\overline{Nu}_{conc,ODg}\, k_{air}\,(T_{g,o} - T_{amb})}{OD_g} \tag{22}$$

the convective heat transfer from the outer glass surface to the ambient is determined by Eq. (23), the corresponding convection HTC, h_{cg} can be calculated using

$$\dot{Q}_{conv,go} = h_{cg} A_{g,o} (T_{g,o} - T_{amb}) \tag{23}$$

The radiation heat transfer coefficients (h_{ra} *and* h_{rg}) are calculated using the measured experimental data of $T_a, T_{g,o}$ *and* T_{amb}. The analytical model described all of the above which is presented in a flow chart in the Fig.5

4. Results and Discussions

4.1. Experimental results on overall heat loss coefficient of inner tube

Experimental investigations are carried out on overall heat loss coefficients using four different annular gap ratios. The experimental data is used to validate the analytical model. The analytical model is used for obtaining the contributions of convection and radiation heat transfer to the total heat loss. Measurement of wall temperatures of absorber tube and glass tube, voltage and current supplied to the absorber tube are noted after the test section reaches steady state. The temperatures are measured at three axial locations which are equidistant from each other. The air in the annular region receives heat from the inner stainless-steel tube. This results in the increase in the temperature of the air between the glass tube and the absorber tube. This leads to the rising of relatively hotter air due to buoyancy effects allowing relatively cooler air to take its place. The rising air encounters the glass tube at the top and loses some of the heat to the ambient through the glass. This makes the air sink to the bottom only to gain heat from the heated stainless-steel tube. The presence of hot air in the upper portion of the annular region results in a relatively higher temperature of the stainless -steel tube as compared to lower temperature.

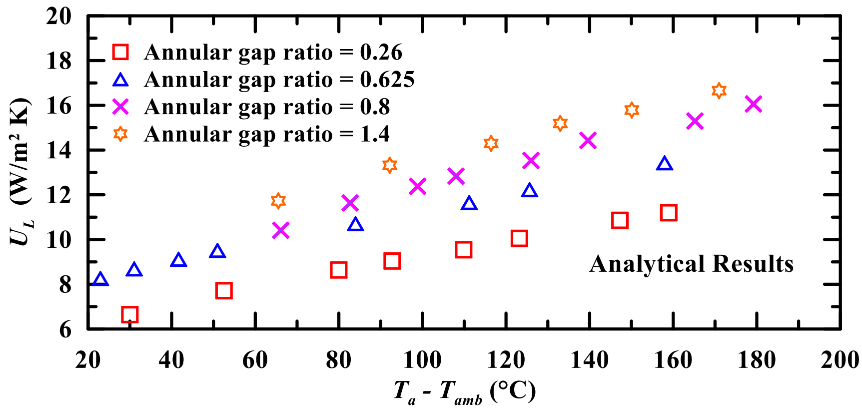

(a)

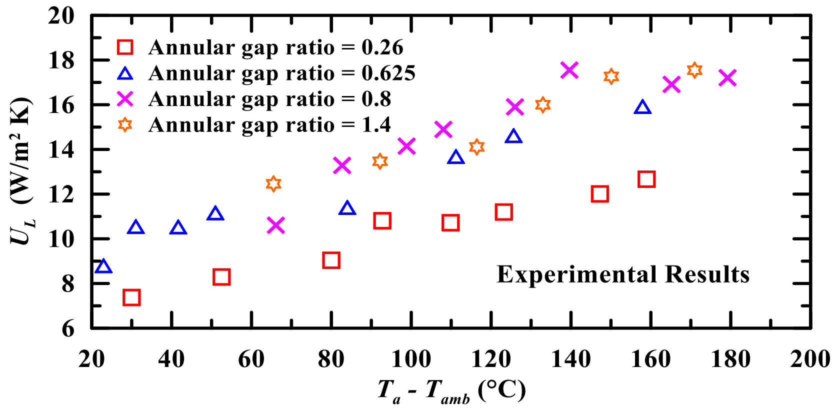

(b)

Fig. 8 Variation of analytical and experimental results of overall HLC with temperature difference within absorber and ambient with different annular gap ratio

The steady state condition, absorber tube temperature increases with increases the heat flux input. It is observed that the individual temperatures at an axial location are close to the average temperature at the same axial location. The other test sections considered for the investigations exhibit similar temperature deviations.

Fig. 8 gives the variation of the overall HTC with the difference in the overall average absorber tube temperature and ambient temperature for all the configurations covered in the present study. The overall HLC increases with the increase in the temperature difference and the experimental data is available in appendix (A). The overall HLC increases with the increase in the annular gap ratio (annular gap non–dimensionalized by the absorber tube diameter ($\delta^* = \delta/OD_a$) for a given temperature difference. Fig. 8(a) and Fig. 8(b) shows the variation of the analytical and experimental result of overall HLC with difference of temperature between average absorber tube and ambient for different annular gap ratio. It is observed that, for minimum annular gap ratio (0.26), the overall HLC is lower and for higher annular gap ratio (1.4), the overall HLC is higher. This is because of accumulation of air inside the annulus region (non-evacuated tube receiver). Table 4 presents the minimum, maximum and average deviation of overall HLC for analytical model with the experiments result. The maximum deviation is within the tolerance limits $\pm 13\%$.

Table 4. Minimum, maximum and average deviations of the analytical overall HLC with the experimental values

Test section	OD_a mm	ID_g mm	Annular gap, mm	Minimum deviation (%)	Maximum deviation (%)	Average deviation (%)
1	25	38	6.5	4.4	16.35	10
2	10	26	8	1.82	17.8	11.2
3	10	38	14	-1.30	8.56	4
4	10	22.5	6.25	6.10	17.66	13

Fig. 9 shows the variation of U_L with temperature difference between average absorber tube and ambient. the results are obtained from the analytical model compared with the experimental results for different gap ratio. The study has been done for four different annular gap ratios or non-dimensionalised gap ratios (0.26, 0.625, 0.8 and 1.4). it is absorved that, the U_L increases with average absorber tube wall temperature because of accumulation of air inside the annulus region (non-evacuated tube receiver). Overall heat loss coefficiet and heat losses are minimum for minimum annular gap ratio (0.26) and maximum for maximum gap ratio (1.4).

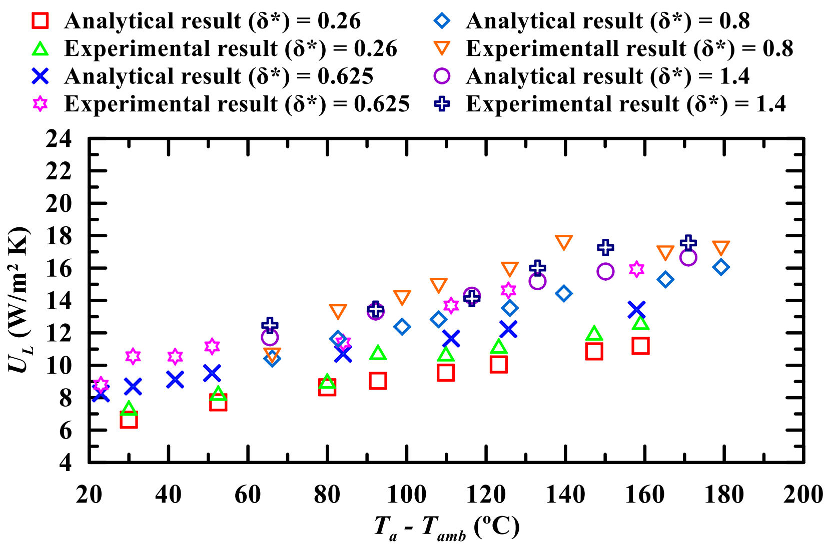

Fig. 9 Comparison of the analytically computed of overall HLC with experimentally measured value for different annual gap ratio

Overall heat loss coefficiet and heat losses are minimum for minimum annular gap ratio (0.26) and maximum for maximum gap ratio (1.4).

4.2 Contribution of different modes of heat transfer to overall heat loss coefficient

The uniform heat flux is supplied to the inner SS tube which is transferred to the glass tube at steady state through natural convection and radiation. Eventually, it dissipated the amount of heat transfer rate to the surroundings from the outer surface of the glass tube through free convection and radiation. The analytical model is established and validated by the experimental results obtained which is shown in the Fig. 9. This model is further utilised to the contribution made by the individual modes of heat transfer to the overall heat loss. Fig. 10(a) and Fig. (b) shows the variation of percentage contribution of heat transfer rate (W) or heat loss with temperature difference between average absorber tube and ambient by free convection and radiation heat transfer mode in the annulus and ambient region. In the annulus region, the convection heat transfer component contribution to the total heat loss is higher than the radiation component.

It can be observed that, in Fig. 10(a) and Fig. 10(b) the percentage contribution of convection heat transfer rate in the annular region ranges between 51% and 74% while radiation heat transfer in annular region ranges from 32% and 48%. For a given configuration, the contribution of free convection in the annular region decreases with increasing absorber tube temperature. This implies that the contribution of the radiation heat transfer to the heat loss in the annular region increases with absorber tube temperature. The convection component contribution in the annular region is higher for the larger annular gap. The increase in the annular gap accommodates more volume of air which implies that more air is available to carry the supplied heat flux by natural convection.

In the Fig. 11(c) and Fig. 11(d) it is observed that, the contribution of radiation heat transfer in the glass tube to ambient region decreases with absorber tube temperature. This implies that contribution of the convection heat transfer to the heat loss in the glass tube to ambient region increases with absorber tube temperature. The reverse trend is observed in the contributions of convection and radiation heat transfer in the glass tube to ambient region. The glass tube to ambient region refers to the region external to the outer glass tube surface. The radiation heat transfer component is higher than the convection heat transfer component in this region. The contribution of the radiation heat transfer to the total heat transfer from the glass tube to the ambient varies between 41% and 58%.

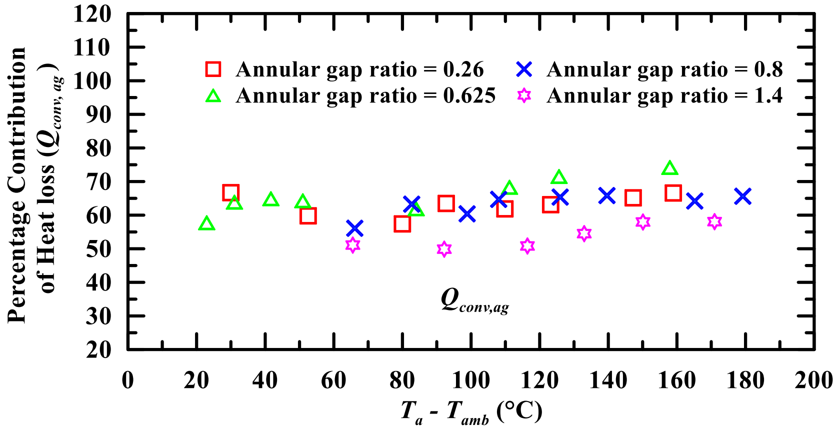

(a)

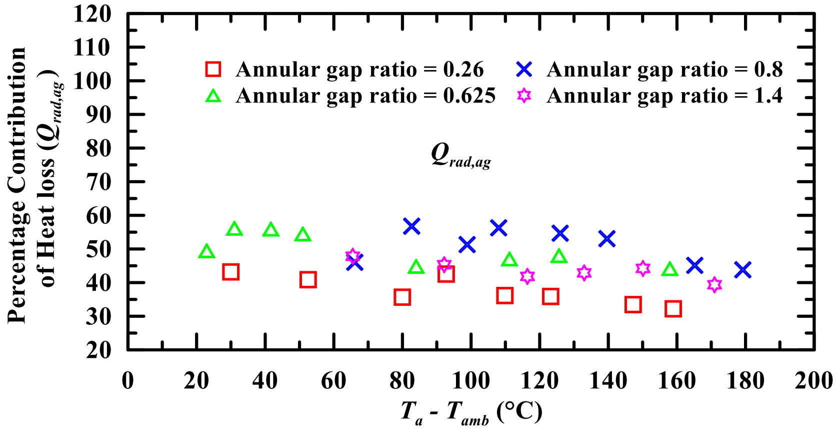

(b)

Fig. 10 Percentage contribution of loss of heat with difference of temperature between absorber tube and ambient

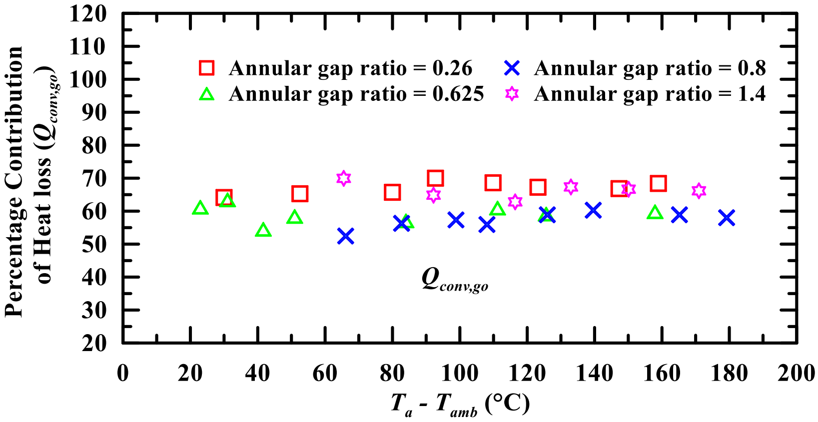

(c)

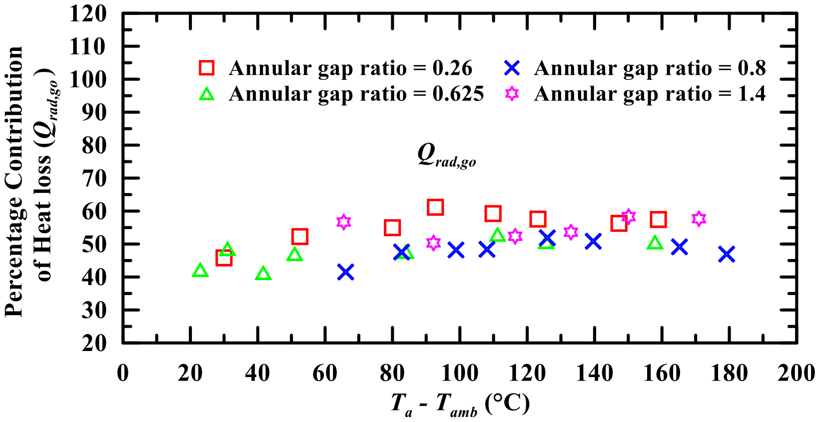

(d)

Fig. 11 Percentage contribution of heat loss modes with varying temperature difference between the absorber tube and ambient

4.3 Empirical correlations for the heat flux and overall heat loss coefficient (U_L)

Correlations for the heat flux (q'') and U_L as a function of temperature difference between average absorber tube and ambient ($T_a - T_{amb}$), annular gap ratio (δ^*) are shown in Eq. (24) and (25).

$$q'' = 3.57\,(T_a - T_{amb})^{1.3}\delta^{*0.206}$$
$$29°C \le (T_a - T_{amb}) \le 180°C,\;\; 0.26 \le \delta^* \le 1.4 \qquad (24)$$

$$U_L = 3.57\,(T_a - T_{amb})^{0.3}\delta^{*0.206}$$
$$29°C \le (T_a - T_{amb}) \le 180°C,\;\; 0.26 \le \delta^* \le 1.4 \qquad (25)$$

The deviations between the Correlations of heat flux and overall heat loss coefficient (U_L) from the Eq. (24) and Eq. (25) with the experimental results is within the tolerance limits $\pm$14.5% and $\pm$15%, respectively.

5. Conclusions

Experiments are carried out to measure the experimental value of overall heat loss coefficient (U_L) in a non – evacuated tube receiver. The receivers tested in this work are concentric glass tubes with stainless steel tube as the absorber tube enclosed concentrically in a borosilicate glass tube. The inner stainless-steel tube is subjected to uniform heat flux. Different configurations of test sections are obtained by varying the absorber tube diameter and outer glass tube diameter. U_L values obtained for average absorber tube wall temperatures ranging from 50°C to 215°C. The U_L is observed to increase with the average absorber tube temperature. The experimental results of U_L are also compared using non – dimensional annular gap ratio(δ^*). Non-dimensional annular gap ratio calculating based on the outer absorber tube diameter ($\delta^* = \frac{\delta}{OD_a}$). The following results are given below-

1. δ* (δ/OD_a) is more effective for comparing U_L than absolute gap δ.
2. δ* range**:** 0.26 – 1.40**;** minimum U_L at δ* = 0.26.
3. Thermal model (electrical network analogy) validated with experiments**;** 13% average deviation**.**
4. In annular gap: Natural convection = 51 – 74%, Radiation = 26 – 49%.

5. From glass to ambient: Radiation = 42 – 58%**,** convection similar in magnitude.
6. Correlation developed for heat flux and U_L using absorber – ambient temperature difference and δ*.

Therefore, heat loss by convection in annular region can be reduced by reducing the non – dimensional annular gap in non–evacuated tube receivers. The radiation component may be reduced by the use of air stable selective coatings on the surface of absorber tube. In the present case, Pyro-mark solar selective coating materials is used.

Acknowledgements
Authors thank Mr. Rahul Shirsat for his technical support in building the experimental setup. This research did not receive funding from public, commercial, or non-profit sectors.

References

[1] Häberle A, Zahler C, Lerchenmüller H, Mertins M, Wittwer C, Trieb F, Dersch J. The Solarmundo line focussing Fresnel collector. Optical and thermal performance and cost calculations. In Proceedings of SolarPACES Int Symp 2002.

[2] Singh PL, Sarviya RM, Bhagoria JL. Thermal performance of linear Fresnel reflecting solar concentrator with trapezoidal cavity absorbers. Appl Energy 2010;87:541–50. doi:10.1016/j.apenergy.2009.08.019.

[3] Zhu G, Wendelin T, Wagner MJ, Kutscher C. History, current state, and future of linear Fresnel concentrating solar collectors. Sol Energy 2014;103:639–52. doi:10.1016/j.solener.2013.05.021.

[4] Moghimi MA, Craig KJ, Meyer JP. Optimization of a trapezoidal cavity absorber for the Linear Fresnel Reflector. Sol Energy 2015;119:343–61. doi:10.1016/j.solener.2015.07.009.

[5] Singh PL, Sarviya RM, Bhagoria JL. Heat loss study of trapezoidal cavity absorbers for linear solar concentrating collector. Energy Convers Manag 2010;51:329–37. doi:10.1016/j.enconman.2009.09.029.

[6] Larsen SF, Altamirano M, Hernandez A. Heat loss of a trapezoidal cavity absorber for a linear Fresnel reflecting solar concentrator. Renew Energy 2012;39:198–206. doi:10.1016/j.renene.2011.08.003.

[7] Facão J, Oliveira AC. Numerical simulation of a trapezoidal cavity receiver for a linear Fresnel solar collector concentrator. Renew Energy 2011;36:90–6. doi:10.1016/j.renene.2010.06.003.

[8] Sahoo SS, Singh S, Banerjee R. Analysis of heat losses from a trapezoidal cavity used for Linear Fresnel Reflector system. Sol Energy 2012;86:1313–22. doi:10.1016/j.solener.2012.01.023.

[9] Shanmugapriya B, Reddy KS, Sundarajan T. Performance investigation of linear evacuated absorber of 2-stage solar Linear Fresnel Reflector module under non-uniform flux distribution. Int J Low-Carbon Technol 2018;13:92–101. doi:10.1093/ijlct/ctx024.

[10] Reddy KS, Balaji S, Sundararajan T. Heat loss investigation of 125kW th solar LFR pilot plant with parabolic secondary evacuated receiver for performance improvement. Int J Therm Sci 2018;125:324–41. doi:10.1016/j.ijthermalsci.2017.11.006.

[11] Ratzel AC, Hickox CE, Gartling DK. Techniques for reducing thermal conduction and natural convection heat losses in annular receiver geometries. J Heat Transfer 1979;101:108. doi:10.1115/1.3450899.

[12] Gee R, Gaul HW, Kearney D, Rabl A. Long-term average performance benefits of parabolic trough improvements. No. SERI/TR-632-439. Solar Energy Research Inst., Golden, CO (USA) 1980.

[13] Cachafeiro H, Arevalo LF De, Vinuesa R, Lopez-Vizcaino R, Luna M. Analysis of vacuum evolution inside solar receiver tubes. Energy Procedia 2015;69:289–98. doi:10.1016/j.egypro.2015.03.033.

[14] Moffat RJ. Describing the uncertainties in experimental results. Exp Therm Fluid Sci 1988;1:3–17. doi:10.1016/0894-1777(88)90043-X.

[15] Bejan A. Convection Heat Transfer. Fourth ed. John Wiley & Sons, Inc., Hoboken, New Jersey; 2013.

[16] Raithby GD, Hollands KGT. A general method of obtaining approximate solutions to laminar and turbulent free convection problems. Adv in Heat Transf 1975;11:265–315. doi:DOI: 10.1016/S0065-2717(08)70076-5.

[17] Churchill SW, Chu HHS. Correlating equations for laminar and turbulent free convection from a horizontal cylinder. Int J Heat Mass Transf 1975;18:1049–53. doi:10.1016/0017-9310(75)90222-7.

Nomenclature

A_a	Outer surface area of absorber tube	m^2	$A_{g,o}$	Outer surface area of concentric glass tube	m^2
$A_{g,i}$	Inner surface area of concentric glass tube	m^2	C_p	Specific heat at constant pressure	$J/kg\ K$

h_{ra}	Radiation HTC from the absorber tube	W/m^2K
h_{ca}	Convection HTC from the absorber tube	W/m^2K
h_{rg}	Radiation HTC from the concentric glass tube	W/m^2K
h_{cg}	Convection HTC from the concentric glass tube	W/m^2K
ID_a	Inner diameter of absorber tube	m
ID_g	Inner diameter of glass tube	m
I	Current	$Ampere$
k	Materials thermal conductivity	$W/m\,K$
L	Heated length	m
$\overline{Nu}_{conv,Dgo}$	Nusselt number from glass tube to ambient based on glass outer diameter $\overline{Nu}_{conv,Dg,o} = \frac{h_{cg}\,OD_g}{k_{air}}$	$-$
OD_a	Outer diameter of absorber tube	m
OD_g	Outer diameter of glass tube	m
$Pr_{g,o}$	Prandtl number for glass outer tube temperature to ambient $Pr_{g,o} = \frac{\mu_{air}\ C_{P,air}}{k_{air}}$	$-$
$\dot{Q}$	Heat transfer rate	W
$\dot{Q}_{ao}$	HTR from absorber tube to ambient	W
$\dot{Q}_{cg,o}$	Convection HTR from concentric glass tube to ambient	W
$\dot{Q}_{conv,ag}$	Convection HTR between absorber tube and inner surface glass tube	W
$\dot{Q}_{rg,o}$	Radiation HTR from concentric glass tube to ambient	W
$\dot{Q}_{rad,ag}$	Radiation HTR between absorber tube and inner surface of concentric glass tube	W
q'	Heat transfer per unit length	W/m
q''	Heat flux (W/m^2)	W/m^2
R	Thermal resistance	K/W
$Ra_{Dg,o}$	$Ra_{Dg,o} = \frac{g\beta(T_a - T_{amb})OD_g^3}{\gamma^2} \times Pr$	$-$
T_a	Average temperature of absorber tube	K
T_{amb}	Ambience temperature	K
$T_{g,i}$	Inner temperature of glass tube	K
$T_{g,o}$	Outer temperature of glass tube	K
U_L	Overall HLC	W/m^2K
V	Voltage	$Volts$

Greek symbols

α_{air}	Thermal diffusivity of air (m^2/s)
ε_a	Emissivity of absorber tube
ε_g	Emissivity of concentric glass tube
ρ	Density (kg/m^3)
σ	Stefan – Boltzmann constant (5.67×10^{-8} (W/m^2 K^4))
β	Coefficient of volume expansion (1/K)
γ_{air}	Kinematic viscosity of air (m^2/s)
δ	Annular gap (mm) $\left(ID_g - OD_a\right)/2$
δ^*	Annular gap ratio $(\delta)/(OD_a)$

Subscripts

a	Absorber tube
ag	Inner tube to glass
air	Air
amb	Ambient
ao	Inner tube to ambient
$conv$	Convection
g	Glass cover
go	Glass to ambient
i	Inner
o	Outer

Abbreviations

CSP	Concentrating solar power
LFR	Linear Fresnel reflector
HLC	Heat loss coefficient
OHLC	Overall heat loss coefficient (U_L)
HTR	Heat transfer rate
HTF	Heat transfer fluid
PTC	Parabolic trough collector
SS	Stainless steel
AC	Alternating current
DAS	Data acquisition system
SNETR	Single non-evacuated tube receiver
HTC	Heat Transfer coefficient